Iterative Computation of Moment Forms for Subdivision Surfaces

Jan P. Hakenberg
ETH Zürich

Ulrich Reif
TU Darmstadt

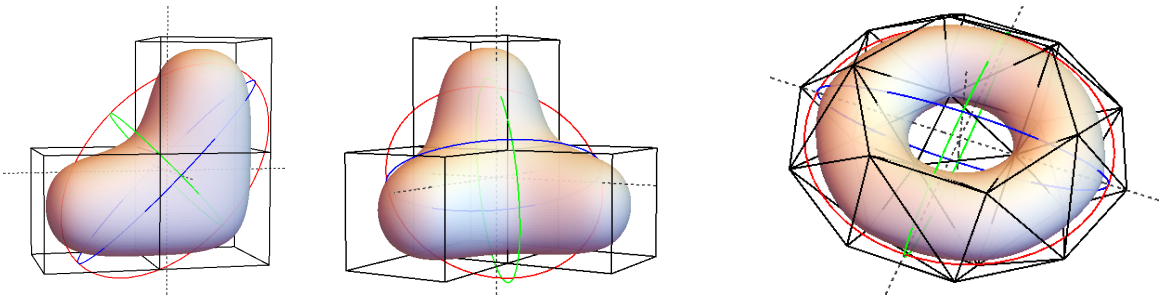

Figure 1: *Solids bounded by Catmull-Clark and Loop subdivision surfaces with centroids indicated by dashed lines, and inertia indicated by the principal axes of the ellipsoid with equivalent inertia. The iterative derivation of multilinear forms determines the moments with unprecedented accuracy.*

Abstract

The derivation of multilinear forms used to compute the moments of sets bounded by subdivision surfaces requires solving a number of systems of linear equations. As the support of the subdivision mask or the degree of the moment grows, the corresponding linear system becomes intractable to construct, let alone to solve by Gaussian elimination. In the paper, we argue that the power iteration and the geometric series are feasible methods to approximate the multilinear forms. The tensor iterations investigated in this work are shown to converge at favorable rates, achieve arbitrary numerical accuracy, and have a small memory footprint. In particular, our approach makes it possible to compute the volume, centroid, and inertia of spatial domains bounded by Catmull-Clark and Loop subdivision surfaces.

Keywords: Stationary subdivision, volume, centroid, inertia.

Concepts: •**Theory of computation** → **Computational geometry;** •**Computing methodologies** → **Shape analysis;**

1 Introduction

Volume, centroid, and inertia are important shape characteristics in 3D modeling and animation. Accurate formulas for the determination of the moments of solids bounded by stationary subdivision schemes have only recently become available. The approach is restricted to the computation of moments of low degree and to subdivision schemes with weight masks of small support.

The iterative methods presented in this publication extend the limits of what is possible. Using the new framework to compute moment forms, solids bounded by subdivision surfaces such as Catmull-Clark or Loop can be designed with exact volume, centroid, and inertia up to machine precision.

The moment formula for solid shapes in the context of subdivision has the following applications: By translation of vertices in the control mesh, limit surfaces can be deformed subject to preservation of volume and centroid of the interior set. If a subdivision surface is the contour of an animated entity with constant mass density, the formulas help to make the motion physically more accurate. In the absence of applied torques, the inertia (second moment) is used to determine motions that preserve angular momentum.

1.1 Related Work

[Peters and Nasri 1997] approximate the moment of solids bounded by [Doo and Sabin 1978] and [Catmull and Clark 1978] surfaces by increasing the level of refinement around non-regular vertices of a mesh. As facets adjacent to non-regular vertices decrease in size, their moment contribution can be approximated using a planar surface patch. The approach requires regular submeshes to have a polynomial parametrization. Moments defined by the Butterfly scheme by [Dyn et al. 1990] are not covered by their framework.

[Schwald 1999] achieves accurate results for solids bounded by the Doo-Sabin algorithm. The moment contribution of a non-regular facet is expressed as a multilinear form in the coordinates of the vertices of the control mesh. In order to compute the form coefficients, the volume contributions of all spline rings are taken into account. This is achieved by eigen-decomposition of the subdivision matrix. The contributions of infinite sequences of scaled eigen-rings form a geometric series. The exact limit of the series is determined algebraically.

[Warren and Weimer 2001] pp. 162–167 calculate the exact area form for the 4-point curve subdivision scheme by [Dubuc 1986]. The derivation is the first application of the homogeneous refinement equation (11) in the literature.

[Hakenberg et al. 2014] derive the exact moment forms for facets adjacent to non-regular vertices as well as sharp creases from the general refinement equation (7). The limitation of the approach is the size of the non-sparse linear systems that are solved to determine the coefficients of the tensors. As the complexity of the subdivision scheme, patch topology, and degree of moment grows, the corresponding linear system becomes intractable to store in memory and solve by Gaussian elimination. For instance, the inertia form for a quad facet adjacent to a vertex of valence 5 in a Catmull-Clark mesh has 86346 coefficients.

1.2 Contributions

We build upon the work of [Hakenberg et al. 2014] by introducing two iterative methods that approximate the coefficients of the moment forms up to arbitrary numerical precision. The first method is the power iteration that determines the form as an eigenvector associated with the largest eigenvalue of a linear system. The second

iteration type is a geometric series. Eigen-analysis guarantees that the iterations converge at favorable rates for standard subdivision schemes so that building the matrix of the linear system becomes unnecessary.

Catmull-Clark surfaces are the de facto standard for 3D modeling in the entertainment industry. Our approach allows to calculate volume, centroid, and inertia of solids bounded by these surfaces with unprecedented accuracy and minimal computational effort.

2 Preliminaries

The moment $E_{p,q,r}(\Omega)$ of a bounded set $\Omega \subset \mathbb{R}^3$ for non-negative integers p, q, r is defined as the integral

$$E_{p,q,r}(\Omega) := \int_\Omega x^p y^q z^r \mathrm{d}x\mathrm{d}y\mathrm{d}z. \tag{1}$$

The degree d is defined as $d := p + q + r$. Moments of low degree d have interpretations as

$$\begin{aligned}
\text{volume}(\Omega) &= E_{0,0,0}(\Omega),\\
\text{centroid}(\Omega) &= \frac{1}{\text{volume}(\Omega)}(E_{1,0,0}(\Omega), E_{0,1,0}(\Omega), E_{0,0,1}(\Omega)),\\
\text{inertia}(\Omega) &= (E_{2,0,0}(\Omega), E_{0,2,0}(\Omega), E_{0,0,2}(\Omega),\\
&\qquad E_{1,1,0}(\Omega), E_{0,1,1}(\Omega), E_{1,0,1}(\Omega)).
\end{aligned}$$

The mass density is assumed to be constant across the domain Ω.

The divergence theorem with vector field $G : \mathbb{R}^3 \to \mathbb{R}^3$ as $G(x, y, z) = (\frac{1}{p+1}x^{p+1}y^q z^r, 0, 0)$, and div $G = x^p y^q z^r$ reformulates (1) to an integral over the boundary $\partial\Omega$

$$E_{p,q,r}(\Omega) = \frac{1}{p+1}\int_{\partial\Omega} x^{p+1} y^q z^r \vec{n}_x \mathrm{d}A, \tag{2}$$

where $\vec{n}_x$ denotes the x-component of the surface normal.

2.1 Multilinear Forms

Let $\mathcal{M}$ be an orientable mesh of control points. According to [Schwald 1999] and [Hakenberg et al. 2014], the moment of the set Ω bounded by the subdivision limit surface $\partial\Omega = S^\infty(\mathcal{M})$ is computed as a sum over all facets of the mesh

$$E_{p,q,r}(\Omega) = \sum_{f\in\mathcal{M}} E_{p,q,r}(f). \tag{3}$$

The contribution of the facet f to the global moment is

$$E_{p,q,r}(f) = \frac{1}{p+1} M_d^{\tau(f)} \cdot \underbrace{\mathbf{x}.\cdots.\mathbf{x}}_{p+1\text{-times}} \cdot \underbrace{\mathbf{y}.\cdots.\mathbf{y}}_{q\text{-times}} \cdot \underbrace{\mathbf{z}.\cdots.\mathbf{z}}_{r\text{-times}} . \mathbf{y}.\mathbf{z}. \tag{4}$$

The control points that determine the surface patch associated to f are arranged into the coordinates vectors **x**, **y**, **z**. For instance, in a Catmull-Clark control mesh, each quad is a facet. The control points in the one ring of the quad determine the surface patch.

The tensor $M_d^{\tau(f)}$ depends on the topology $\tau(f)$ of the facet, and the degree d of the moment. [Peters and Nasri 1997] establish that the coefficients of the tensor $M_d^{\tau(f)}$ have the following integral expression

$$\begin{aligned}
(M_d^{\tau(f)})_{i_1,\ldots,i_{d+1},j,k} &=\\
&\int_D b_{i_1}\cdots b_{i_{d+1}}(\partial_s b_j \partial_t b_k - \partial_t b_j \partial_s b_k)\mathrm{d}s\mathrm{d}t.
\end{aligned} \tag{5}$$

For quad-based subdivision schemes the domain is $D = [0, 1]^2$, and for triangle based schemes $D = \{(s, t) \in \mathbb{R}^2 | 0 \le s, t \wedge s+t \le 1\}$. The basis function $b_i : D \to \mathbb{R}$ is associated to control point i.

For surfaces that consist entirely of B-spline, or Bézier-Bernstein patches, [Gonzalez-Ochoa et al. 1998] integrate (5) symbolically in order to yield the exact tensor coefficients. For facets in subdivision meshes that are adjacent to non-regular vertices, the basis functions typically do not have a closed-form expression.

2.2 Recursive Formulation

We summarize the derivation given in [Hakenberg et al. 2014]. One round of subdivision partitions a facet $f \in \mathcal{M}$ into a number of smaller facets $f_h := S_h(f)$. For standard surface schemes $h \in \{1, 2, 3, 4\}$, see Figures 3 and 4, but this is not a requirement. The contribution $E_{p,q,r}(f)$ to the global moment of Ω is identical to the total contribution of the subdivided parts

$$E_{p,q,r}(f) = \sum_h E_{p,q,r}(S_h(f)). \tag{6}$$

Substituting $\mathbf{x} \leftarrow S_h.\mathbf{x}$, $\mathbf{y} \leftarrow S_h.\mathbf{y}$, and $\mathbf{z} \leftarrow S_h.\mathbf{z}$ in (4) to expand the rhs of (6) yields the general tensor equation independent of control points

$$M_d^{\tau(f)} = \sum_h M_d^{\tau(f_h)}[S_h]. \tag{7}$$

The tensor transformation $M[S]$ is shorthand for the basis transformation along each dimension of tensor M with S, i.e.

$$(M[S])_{i_1,\ldots,i_m} := \sum_{j_1,\ldots,j_m} M_{j_1,\ldots,j_m} S^{j_1}_{i_1}\cdots S^{j_m}_{i_m}.$$

The matrix S does not have to be square.

In order to solve the coefficients of $M_d^{\tau(f)}$, equation (7) is written as a linear system $m = c + A.m$. Matrix A encodes the linear relationship between the sought coefficients of $M_d^{\tau(f)}$ that make up vector m.

In case of homogeneous refinement, i.e. $\tau(f) = \tau(f_h)$ for all h, it follows that vector $c = 0$. Then, the problem is reduced to identifying m as an eigenvector to eigenvalue 1 of matrix A

$$m = A.m. \tag{8}$$

Once established, the eigenvector m has to be scaled to the proper length in a calibration step using a configuration of control points **x**, **y**, **z** for which the moment $E_{p,q,r}(f)$ of the surface patch is known analytically. The calibration procedure is detailed in [Hakenberg et al. 2014] and [Hakenberg and Reif 2016b].

In case of non-homogeneous refinement, i.e. $\tau(f) \neq \tau(f_h)$ for at least one h, vector c aggregates the contribution of the subdivided facets for which the moment forms $M_d^{\tau(f_h)}$ are already known. The resulting linear system is of the form

$$(I - A).m = c. \tag{9}$$

For non-regular vertices, the facet topology $\tau(f)$ typically appears once in the sum of the rhs of (7), see Figure 4. Then, the system matrix $A = \otimes^{d+3} S$ is the $(d + 3)$-fold Kronecker product of the square subdivision matrix S. S maps the coordinates of the control points associated to facet f to those of the subdivided non-regular facet f_h with $\tau(f) = \tau(f_h)$. The eigenvalues of A follow from the eigenvalues of S. For common subdivision schemes, A has

eigenvalue 1 with multiplicity 1, and all other eigenvalues λ with $|\lambda| < 1$. That means $I - A$ is rank deficient by 1. The nullspace of $I - A$ corresponds to a symmetric tensor. But m is skew in the last two dimensions as seen from (5), that means m follows uniquely from (9).

2.3 Tensor Symmetry

When arranging the coefficients of $M_d^{\tau(f)}$ into a vector m, redundant entries stemming from tensor symmetries should be omitted in order to reduce the complexity of the linear system.

Two symmetry relations are intrinsic to the inner product (5): Invariance under permutation of the first $d+1$ indices

$$(M_d^{\tau(f)})_{i_1,\dots,i_{d+1},j,k} = (M_d^{\tau(f)})_{\text{sort}(i_1,\dots,i_{d+1}),j,k},$$

and skew symmetry in the last two dimensions

$$(M_d^{\tau(f)})_{i_1,\dots,i_{d+1},j,k} = -(M_d^{\tau(f)})_{i_1,\dots,i_{d+1},k,j}.$$

Permutations of control points under which the image of the surface patch is invariant also contribute to tensor symmetries. For instance, rotation ρ of control point indices of a regular facet results in the same tensor coefficient

$$(M_d^{\tau(f)})_{i_1,\dots,i_{d+3}} = (M_d^{\tau(f)})_{\rho(i_1),\dots,\rho(i_{d+3})}.$$

Mirroring σ of control point indices of a facet along an axis of mirror symmetry flips the sign

$$(M_d^{\tau(f)})_{i_1,\dots,i_{d+3}} = -(M_d^{\tau(f)})_{\sigma(i_1),\dots,\sigma(i_{d+3})}.$$

For degree $d = 0$, one may additionally assume that the trilinear form is alternating, i.e.

$$(\hat{M}_0^{\tau(f)})_{i,j,k} = \frac{1}{6} \sum_{\pi \in \mathcal{S}_3} \text{sign}(\pi) (M_0^{\tau(f)})_{\pi(i,j,k)}, \qquad (10)$$

where $\mathcal{S}_3$ is the permutation group of order $3! = 6$. [Hakenberg and Reif 2016b] treat alternating volume forms for refinable basis functions b_i of which subdivision surfaces are a special case.

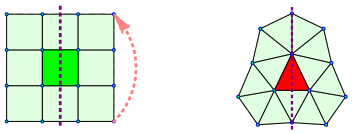

Figure 2: *Rotation (pink arrow) and mirror (purple axis) symmetries of facets f.*

Examples The surface patch associated to a regular Catmull-Clark quad facet f is determined by 16 control points. The left diagram in Figure 2 illustrates the symmetries. The moment contribution of the facet is invariant up to sign under rotation and mirroring of the control points. The number of unique coefficients in the centroid form M_1^4 is bounded by 2048.

The surface patch associated to a Loop triangular facet f with a non-regular vertex of valence $\tau(f) = 7$ is determined by 13 control points. The moment contribution of the facet is invariant up to sign under mirroring of the control points across the axis through the non-regular vertex, see the right diagram in Figure 2. The number of unique coefficients in the inertia form M_2^7 is bounded by 17592.

3 Iteration of Forms

Despite taking coefficient symmetries in $M_d^{\tau(f)}$ into account, the linear systems (8) and (9) may still be too large to build and determine m. Moreover, the system matrix is typically non-sparse and has a large condition number. Memory constraints and loss of numerical accuracy prevent the application of Gaussian elimination.

In this section, we argue that the power iteration and the geometric series are feasible methods to approximate the moment forms. In the subsequent treatment, the degree d and facet topology $\tau(f)$ are fixed. We drop these two indices to simplify the notation.

3.1 Homogeneous Refinement

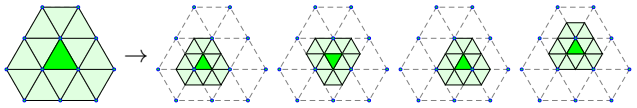

Figure 3: *Subdivision of a regular Loop facet f into f_h for $h \in \{1,2,3,4\}$. S_h are matrices of dimension 12×12 that map the coordinates of the control points in the 1-ring of f to the control points of f_h.*

In case of homogeneous refinement, all moment forms in (7) are identical. The equation simplifies to

$$M = \sum_h M[S_h]. \qquad (11)$$

The system of linear equations is of the form $m = A.m$. An eigenvector m is approximated by the power iteration, if 1 is the largest eigenvalue of matrix A, see [von Mises and Pollaczek-Geiringer 1929]. The smaller the subdominant eigenvalue of A, the faster the convergence of the iteration.

We are not aware of a method to deduce the eigenvalues of A directly from the collection of subdivision matrices S_h. For the subdivision schemes that we investigated, the largest eigenvalue of matrix A is 1. For degree $d = 0$, and assuming that M is an alternating trilinear form (10), the multiplicity of eigenvalue 1 is 1. For $d \in \{1,2\}$, the multiplicity is 2. For Doo-Sabin, Loop, and Catmull-Clark subdivision and $d \in \{0,1,2\}$ the eigenvalues of A were experimentally determined to be of the form 2^{-2n} for $n \in \{0,1,2,...\}$. For the Butterfly scheme with tension parameter $w = 1/16$ and $d = 0$, the set of eigenvalues $\{1, 1/4, 3/32, 1/16, \dots\}$ contains values outside of this pattern.

The construction of matrix A is not required to perform the power iteration. In tensor notation, the sequence is equivalent to

$$\begin{aligned} \tilde{M}_0 &:= \pi(\text{random}) \\ M_k &:= \tilde{M}_k / ||\tilde{M}_k|| \\ \tilde{M}_{k+1} &:= \pi\left(\sum_h M_k[S_h]\right), \end{aligned} \qquad (12)$$

which is more memory efficient. Coefficient symmetries as derived in Section 2.3 are enforced by a linear projection π in between iteration steps. After the iteration has converged, scaling of the form $M = \mu \lim_{k\to\infty} M_k$ with an appropriate factor $\mu \in \mathbb{R}$ is performed analogous to the calibration of eigenvector m in (8).

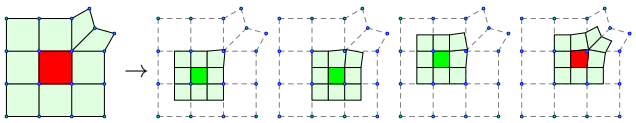

Figure 4: *Subdivision of a Catmull-Clark facet f with a vertex of valence $\tau(f) := 5$ into f_h for $h \in \{1,2,3,4\}$. S_1, S_2, S_3 are 16×18 matrices, S_4 is of dimension 18×18.*

3.2 Non-Homogeneous Refinement

For a facet adjacent to a non-regular vertex, (7) simplifies to

$$M = C + M[S]. \tag{13}$$

The tensor $M = M_d^{\tau(f)}$ is unknown. Square matrix S maps the coordinates of the control points that support f to the control points of f_h with $\tau(f) = \tau(f_h)$. C is the constant tensor aggregated from the known terms. The eigenanalysis of the linear system (9) carried out in Section 2.2 permits to write m as the geometric series

$$m = (I - A)^{-1}.c = \lim_{k\to\infty} \sum_{i=0}^{k} A^i.c.$$

In tensor notation, the geometric series is computed as

$$\begin{aligned} M_0 &:= C \\ M_{k+1} &:= C + M_k[S] \end{aligned} \tag{14}$$

with $M = \lim_{k\to\infty} M_k$. The subdominant eigenvalue of A is the subdominant eigenvalue λ of S. The smaller $|\lambda|$, the faster the convergence, see Figure 6.

4 Summary

The moment forms $M_d^{\tau(f)}$ for a specific subdivision scheme have to be derived only once. Subsequently, the tensors apply universally to any closed, orientable control mesh $\mathcal{M}$ using (3) and (4). The methods to derive the forms are selected based on the type of basis functions, number of coefficients of $M_d^{\tau(f)}$, and requirements on accuracy. In the following overview, methods 1–3 solve the homogeneous refinement equation (11), whereas methods 4–5 solve the non-homogeneous refinement equation (13).

1 Symbolic Integration The basis functions that parametrize regular surface patches of Doo-Sabin and Catmull-Clark surfaces are polynomials. [Peters and Nasri 1997] compute the moment form for arbitrary degree d by explicit integration of (5).

2 Nullspace and Calibration For the Loop, and Butterfly subdivision schemes, the basis functions of the regular facet are not readily available. (8) is rewritten to $(I - A).m = 0$. The nullspace of matrix $I - A$ can be computed algebraically. For Loop's algorithm, the size of matrix A is 43, 874, 4032 squared for $d = 0, 1, 2$ respectively, see [Hakenberg et al. 2014]. For the volume form of the Butterfly scheme, the size of matrix A is 508 squared, see [Hakenberg and Reif 2016b]. Subsequent calibration of the eigenvector m yields the exact, rational tensor coefficients.

3 Power Iteration The regular patch of the Butterfly scheme depends on 29 control points. The centroid form is determined by 22194 coefficients. We estimate that the system matrix A has subdominant eigenvalue of $\lambda = 1/4$. We use the power iteration (12) to approximate the tensor. Machine precision in the coefficients is surpassed after few iterations, see Figure 5.

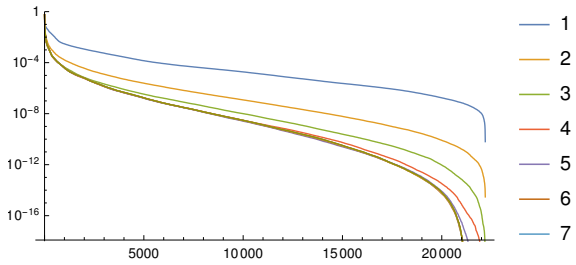

Figure 5: *Coefficients sorted by magnitude of the centroid form M_k for the regular facet of the Butterfly scheme in the power iteration for $k = 1, 2, \ldots, 7$.*

4 Gaussian Elimination [Hakenberg et al. 2014] solve the linear system (9) by Gaussian elimination to obtain the exact moment forms for moderate non-regular vertex valences. If the subdivision weights are rational numbers, the tensor coefficients are also rational. For the Doo-Sabin scheme, the degree is limited to $d \in \{0, 1, 2\}$; for Loop, $d \in \{0, 1\}$; and for Catmull-Clark, $d = 0$. The construction of matrix A for moments beyond the listed degrees is prohibitive due to the large number of form coefficients.

5 Geometric Series We use the tensor iteration (14) to approximate the inertia forms for the Loop scheme, as well as the centroid and inertia forms for Catmull-Clark surfaces and moderate vertex valences $\tau(f)$. The collection of tensors is computed within a day using an implementation in *Mathematica*. The memory footprint of the iteration is low, since only the tensor M_k needs to be stored. The numerical accuracy of the coefficients increases with each iteration step. Figure 6 shows the rate of convergence.

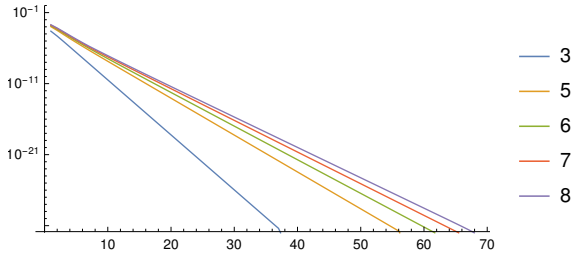

Figure 6: *Convergence of Catmull-Clark inertia forms for non-regular valences up to 8. The slope is determined by the subdominant eigenvalue λ of the subdivision matrix: For vertex valence 3, $\lambda \approx 0.41$; for vertex valence 8, $\lambda \approx 0.61$. Machine precision in the form coefficients is surpassed after no more than 50 iteration steps.*

5 Future Work

We plan to investigate the use of the iterative methods to calculate inner products different from (5). Such inner products arise for instance when modeling a solution space to elliptic partial differential equations.

Acknowledgements

The authors thank Brian Paden for his suggestions that led to the improvement of the article.

References

CATMULL, E., AND CLARK, J. 1978. Recursively generated b-spline surfaces on arbitrary topological meshes. *Computer-Aided Design 10* (Nov.), 350–355.

DOO, D., AND SABIN, M. 1978. Behaviour of recursive division surfaces near extraordinary points. *Computer-Aided Design 10*, 356–360.

DUBUC, S. 1986. Interpolation through an iterative scheme. *Journal of Mathematical Analysis and Applications 114*, 185–204.

DYN, N., LEVIN, D., AND GREGORY, J. 1990. A butterfly subdivision scheme for surface interpolation with tension control. *ACM Transactions on Graphics 9*, 160–169.

GONZALEZ-OCHOA, C., MCCAMMON, S., AND PETERS, J. 1998. A butterfly subdivision scheme for surface interpolation with tension control. *ACM Transactions on Graphics 17*, 143–157.

HAKENBERG, J., AND REIF, U., 2016. Iterative computation of moment forms for subdivision curves and surfaces. https://www.youtube.com/watch?v=oEuOJo1fgGg.

HAKENBERG, J., AND REIF, U. 2016. On the volume of sets bounded by refinable functions. *Applied Mathematics and Computation 272*, 1 (Jan.), 2–19.

HAKENBERG, J., REIF, U., SCHAEFER, S., AND WARREN, J., 2014. On moments of sets bounded by subdivision surfaces. http://vixra.org/abs/1408.0070.

LOOP, C. 1987. *Smooth subdivision surfaces based on triangles*. Master's thesis, University of Utah.

PETERS, J., AND NASRI, A. H. 1997. Computing volumes of solids enclosed by recursive subdivision surfaces. *Computer Graphics Forum 16*, 89–94.

SCHWALD, B. 1999. *Exakte Volumenberechnung von durch Doo-Sabin-Flächen begrenzten Körpern*. Master's thesis, Universität Stuttgart.

VON MISES, R., AND POLLACZEK-GEIRINGER, H. 1929. Praktische verfahren der gleichungsauflösung. *Zeitschrift für Angewandte Mathematik und Mechanik 9*, 152–164.

WARREN, J., AND WEIMER, H. 2001. *Subdivision Methods for Geometric Design: A Constructive Approach*. Morgan Kaufmann.